



Developing Geopolymer Composites as Repair Mortars for Damaged Ancient Egyptian Wall Paintings in Rock Tombs

Hussein H. Marey Mahmoud*

*Department of Conservation, Faculty of Archaeology, Cairo University, 12613 Giza, Egypt



CrossMark

Abstract

This research aims to find out applicable restoration mortars that based mainly on an alkali-activated fly ash geopolymer (GP) mixed with an ethyl silicate polymer or hydrated lime to repair damaged ancient Egyptian wall paintings. Further, the produced composites can be used to repair geotechnical defects in the rock tombs. Technically, the geopolymer is formed by the activation reaction of aluminosilicate materials with an alkali solution. The produced geopolymer was observed by a high resolution field-emission scanning electron microscope (HR-FESEM). Laboratory models were prepared and studied by several methods and tests. The apparent porosity, water absorption, bond and compressive strength, shrinkage, viscosity and the flow rate were measured and evaluated. More, the microscopic characteristics and hydrophobicity of the mortars were analyzed. Further, the stability of the studied samples was assessed against thermal ageing and salt weathering. Well, the physical-mechanical improvements and workability of the tested geopolymer mortars proved their efficiency for restoration purposes such as filling missing parts, repairing the rock defects and as injection grouts for the detached plaster layers.

Keywords: Damaged wall paintings; Fly ash; Geopolymer; Repair mortar; Accelerated ageing; HR-FESEM; Hydrophobicity.

1. Introduction

In ancient Egypt, plastering the rock tombs walls was a common technique. The main purpose of the plaster layers is to refine the rough rock surface (Fig. 1) [1]. Gypsum, mud and lime plasters were applied in different chronological periods. In case of very poor geological structures, the rock joints and voids were first filled up with stone fractions mixed with mud mortar. Frequently, mud plaster was used in the ancient Egyptian rock tombs. This plaster is composed of clay matrix together with plant fibers and a siliceous filler [2]. In some cases, lime, or in all probability, powdered limestone, was added to the components of the plaster. In some Theban tombs, another coating made of 'Hib' (a clayey limestone occurred in the geological structure of the area), powdered limestone and sand, was applied on the coarse mud plaster. Examples for this technique were reported in many tombs such as TT277, TT278, TT175, etc. In case of high quality stones, creating raised or raised-sunken reliefs was applied. Alternatively, high quality stones were collected from another quarry to perform the desired reliefs. The ancient Egyptian rock tombs are suffering from different geotechnical problems. Many forms of structural damage such as joints, cracks and ceilings failure

were documented. Due to their low durability, plasters and reliefs are suffering from several forms of damage such as cracks, disintegration, detachments and the complete loss [3–5]. The restoration process of the damaged heritage materials is a critical issue for conservators. Studies have reported aesthetic alterations of the mud plasters due to some polymeric treatments. Further, a few attention was given to evaluate compatible mortars for plaster restoration. The "geopolymer" introduces a wide group of alkali activated aluminosilicate compounds. The activation process leads to the formation of a 3D polymeric cross-linked gel microstructure [6]. Geopolymer is usually originating from geological materials (e.g. kaolin) or from industrial by-products (e.g. fly ash). Fly ash (FA) is widely used to produce different geopolymers. Fly ash appears as very fine grey granulates and usually produced as by-product of power stations and industrial processes. The pozzolanic behaviour of fly ash depends on components of SiO₂, Al₂O₃ and Fe₂O₃ [7]. The polymerization process is occurred through an alkali activation of aluminosilicates by sodium hydroxide (NaOH) or sodium silicate (Na₂ SiO₃) [8]. In the manufacturing process of the geopolymer, the alkali reaction causes the

*Corresponding author e-mail: marai79@hotmail.com; marai79@cu.edu.eg (H. Marey Mahmoud).

Receive Date: 07 January 2022, Revise Date: 19 February 2022, Accept Date: 23 February 2022

DOI: 10.21608/EJCHEM.2022.115117.5220

©2022 National Information and Documentation Center (NIDOC)

dissolution, partially or completely, of the aluminosilicate structure to form solutions of silica and alumina [9]. Continuously, the water molecules in the aluminosilicate structure are leached out and the oxygen atoms are linked together to form a stable amorphous matrix [10]. Since the production of geopolymers is based on reusing natural raw materials (such as rice husk ash, fly ash, metakaolin, etc.) or through recycling industrial waste, therefore, the environmental sustainability is acquired.

Well, few studies were directed to evaluate the possible application of geopolymers for cultural heritage preservation. The study of Clausi et al. [11] showed the efficiency of metakaolin-based geopolymers for the potential treatment of stone structures. Ricciotti et al. [12] studied the compatibility of a geopolymer composite made of metakaolin and epoxy resin for restoration purposes. Also, Pagnotta et al. [13] reported the super workability of a metakaolin geopolymer which was activated with potassium silicate and sodium hydroxide. The research of Occhipinti et al. [14] approved excellent chemical and mechanical properties obtained by using a pumice and metakaolin based-geopolymer in restoration of historical monuments. In a recent approach, El Khomsi et al. [15] presented the competence of a coating composed of metakaolin, local clays and sand as suitable formula for restoration.

With respect to the chemical and mineralogical composition of the produced geopolymers, the aluminosilicate structure provides desirable qualifications and compatibility to the archaeological wall plasters and reliefs. More, the physical and mechanical advancements of the repair mortars and injection grouts made of these materials present another advantage. For this, the present research aims to formulate a composite made of geopolymer and ethyl silicate-based polymer or hydrated lime as repair mortars and grouts. Consequently, to evaluate their positive characteristics for restoration purposes and stabilizing the geotechnical problems of the ancient Egyptian rock tombs.

2. Materials and methods

2.1. Materials

To prepare the studied composites, several materials and chemicals were used. Fly ash was provided from Sika Egypt Co., Cairo. As described in the technical sheet of the product, the fine FA powder is formed from spherical particles of alumina silicate pozzolan. An alkali activator of sodium hydroxide (NaOH) ACS reagent ($\geq 97.0\%$ anhydrous pellets) was purchased from Sigma-Aldrich (Egypt office). A ready-to-use colourless

to yellowish product of SILRES® BS OH 100 (tetraethyl orthosilicate-TEOS, approx. 100 wt. %) was purchased from CTS srl company, Italy. More, hydrated or slaked lime (portlandite $\text{Ca}(\text{OH})_2$, $85\pm 1\%$) was obtained as dry fine white powder from 'Magnesium Egypt Co'. A grout plasticizer of sodium gluconate ($\text{C}_6\text{H}_{11}\text{NaO}_7$) or D-Gluconic acid sodium in a powder form (purity of 98% min, $\text{pH}=6.2-7.5$) was purchased from Sigma-Aldrich (Egypt office).



Figure 1. (Up) Stratigraphic structure of a wall painting, example from the Theban tomb TT278, (Bottom) wide crack and structural defects of the ceiling, Theban tomb TT192.

2.1.1. Preparation of the geopolymer/composites

First, the geopolymer was prepared through activating an amount of fly ash by 45% sodium hydroxide (NaOH) for 2-3 minutes. An amount of water was added to obtain the required volume. Later, 10% by weight of SILRES® BS OH 100 was added to the geopolymer followed by a stirring process, at 450 rpm for 3 minutes. Actually, this achieves the possibility to create an intra-molecular joining action between the geopolymer gel units and the ethyl silicate structure as proposed by Roviello et al. [16]. Then, the formula was casted into silicon moulds and kept for two weeks at the room temperature to reach the final curing. For the experimental section, a number of cubes was made of the produced geopolymer without any additives. Also, another formula was prepared with the addition of hydrated lime portions (geopolymer, 3 parts and hydraulic lime, 1 part, by weight).

2.2. Analytical methods

2.2.1. Optical microscopy

A digital mobile USB microscope "DNT model" was used to record the physical appearance and the inner microstructure of the tested mortars. The

images were captured with a 5.0 megapixel digital camera under magnifications of 10x and up to 200x.

2.2.2. Field-emission scanning electron microscope (FE-SEM)

The morphological appearance of the archaeological plaster sample, the raw fly ash and the produced geopolymer was analyzed using a high-resolution field-emission scanning electron microscope (FE-SEM) ("Model Philips Quanta FEG 250, Netherlands"). The attached EDX analyzer was operated at an accelerating voltage of 20 kV. For the fly ash samples, a few portion of FA particles was stucked onto a double-sided tape to allow a good investigation of the external surface morphology. The investigations were performed at the Central laboratory of the "National Research Centre of Egypt (NRC)".

2.2.3. X-ray fluorescence (XRF)

The detailed chemical composition of the fly ash samples was determined by a "Phillips PW2400" X-ray fluorescence (XRF) spectrometer.

2.2.4. Physical properties

Water absorption of mortars is considered a key factor for their excellent properties as repair mortars. Three cubes from each formula were prepared and dried in an oven (at a degree of 70 °C) for 24 hrs. The weight of cubes was recorded before and after the complete drying. Then, the cubes were immersed in a water mass box for 24 hrs and their weight was determined. The increase in weight reflects the percentage of the absorbed water. The apparent porosity was measured to evaluate the pores profile of the mortars. The mortar cubes were first weighed in air (WA) and then they were suspended in water to report their weight (WSW). The cubes were soaked in water for 24 hrs and then they were removed and weighted to determine the soaked weight (WS). Values of the apparent porosity were collected according to:

$$\%AP = [(WS-WA)/(WS-WSW)] \times 100\%$$

2.2.5. Test of substrate-mortar bond strength

The tensile bond strength is routinely used to evaluate the properties of repair mortars [17]. The test was performed following the "ASTM C 952-12" standard using a mortar bed joint with a thickness about 5 mm. The samples were left in open air for two weeks to reach the complete curing. The breaking load was recorded and the stress on the mortar joint was calculated.

2.2.6. Compressive strength

Evaluating the compressive strength of mortars is a very common method to record their durability

against crush. Thus, the mortars hardness can be evaluated. The compressive strength test was performed in accordance with "ASTM-C109" through a digital machine.

2.2.7. Shrinkage test

This test is based on the instructions of the "ASTM C 596-96, 1996". The percentage of shrinkage after drying reflects the decrease in length of the cubes during different curing periods.

2.2.8. Viscosity

A "Brookfield DV-E" viscosimeter was used to measure the viscosity of the injection grouts in order to evaluate their workability. After mixing, the values were recorded at rotational speeds up to 100 rpm.

3. Results

3.1. Characterization of the mud-plaster sample

The morphological investigation of a mud plaster sample using the field-emission scanning electron microscope reflected cracking and partial detaching of the plaster (Fig. 2, Up). In the micrograph, fragile plant fibbers are observed. EDX chemical analysis of the sample provided a multi-elemental composition of silicon (Si), aluminium (Al), magnesium (Mg), calcium (Ca), potassium (K) and iron (Fe) (Fig. 2, Bottom). The interpretation of these elements suggests the plaster composition as mud mixed with portions of powdered dolomitic limestone and sand. Local plant fibbers were added as a bonding agent to reinforce the plaster.

3.2. Characterization of fly ash samples

Figure 3 (Up) shows the FE-ESEM morphology of the fly ash particles. The micrograph showed the distribution of multi-size amorphous aluminosilicate cenospheres of hollow spherical and irregular particles. The average size of particles is between 10µm-150µm. The EDX chemical scan of the sample presented silicon, aluminium, iron, calcium and potassium (Fig. 3, Bottom). In addition, the chemical analysis of the sample using the X-ray Fluorescence method (XRF) is given in Table 1.

3.3. Characterization of the formed geopolymer

Figure 4 shows the microstructure of the raw and activated fly ash samples. As observed in Figure 4a, a typical morphological aspect of fly ash is observed. While in Figure 4b, unreacted microspheres filled with very small particles are noticed. After the alkaline activation, compacted matrices, together with unreacted fly ash particles, were detected. This observation indicates the transformation of the amorphous silica and aluminosilicate into a new gel product [18] (Fig.

4c). Figure 5 shows the gel-matrix after the complete curing of the geopolymer-TEOS composite.

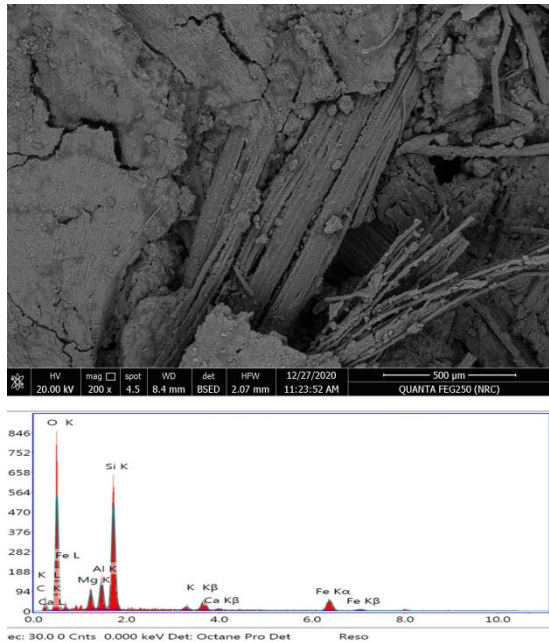


Figure 2. FE-SEM micrograph (Up) and EDX spectrum of the mud plaster sample (Bottom).

Table 1: Chemical composition of the Fly ash (FA) sample using X-ray fluorescence method (XRF)

Chemical	Composition by Weight wt%
SiO ₂	41.33%
Al ₂ O ₃	27.10%
Fe ₂ O	13.26%
CaO	9.08%
MgO	2.03%
K ₂ O	1.94%
SO ₃	1.44%
Na ₂ O	0.97%
LOI	3.01
Si/Al molar ratio	1.52

3.4. Evaluation of the water absorption and apparent porosity

Table 2 and Figure 6 represent the measured values of the water absorption and apparent porosity of the studied mortars. The physical properties of the repair mortars are important parameters. The desired combatability of mortars depends mainly on their physico-chemical behaviour. Water absorption rate was evaluated for the tested mortars. After curing, the geopolymer mortar retained the highest water absorption value (10.5%), while after laboratory salt weathering, it showed a value of (11.9%). In the second level come the specimens of the geopolymer+lime with values of (9.54%) and (10.4%), respectively. But, the geopolymer+TEOS mortar achieved the lowest values, (8.7%) and (9.1%) respectively.

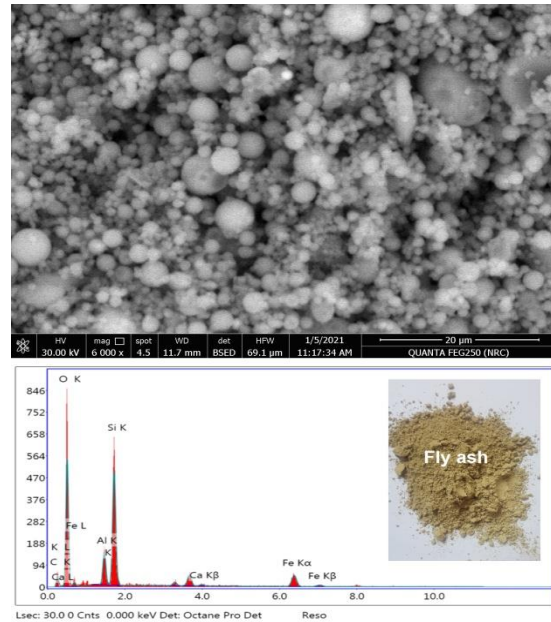


Figure 3. FE-SEM micrograph (Up) and EDX spectrum of the Fly ash (FA) sample (Bottom).

The apparent porosity (AP) expresses the volume of voids, given as percentage, over the total volume of sample. The highest (AP) value was reported for the geopolymer mortars (16.3%), while the lowest value was recorded for the geopolymer+TEOS mortar (12.4%). For the three formulas, salt weathering induced a slight AP increase, reporting 5.2%, 3.2% and 5.3%, respectively. The outer appearance and water-repellent properties of the tested mortars were examined before and after thermal ageing (Fig. 7a, b). A high resistance to wettability was achieved for all specimens (Fig. 7c), and in particular for the geopolymer+TEOS mortar with a contact angle degree reaches 108° (Fig. 7d).

3.5. Evaluation of bond and compressive strength values

Table 3 and Figure 8 show the bond and compressive strength values of the studied mortars. The values of bond strength were measured after 7, 15 and 28 days from the casting time of the mortars. After one week, the three mortars showed almost similar values. Compared to values of the first week, the geopolymer+TEOS mortar showed a remarkable difference in the bond strength (12.9%) after 28 days (Fig. 8a).

In the second level comes the geopolymer+lime mortar, with a percentage of 12.2%. Well, the setting time of mortars influenced positively the measured values.

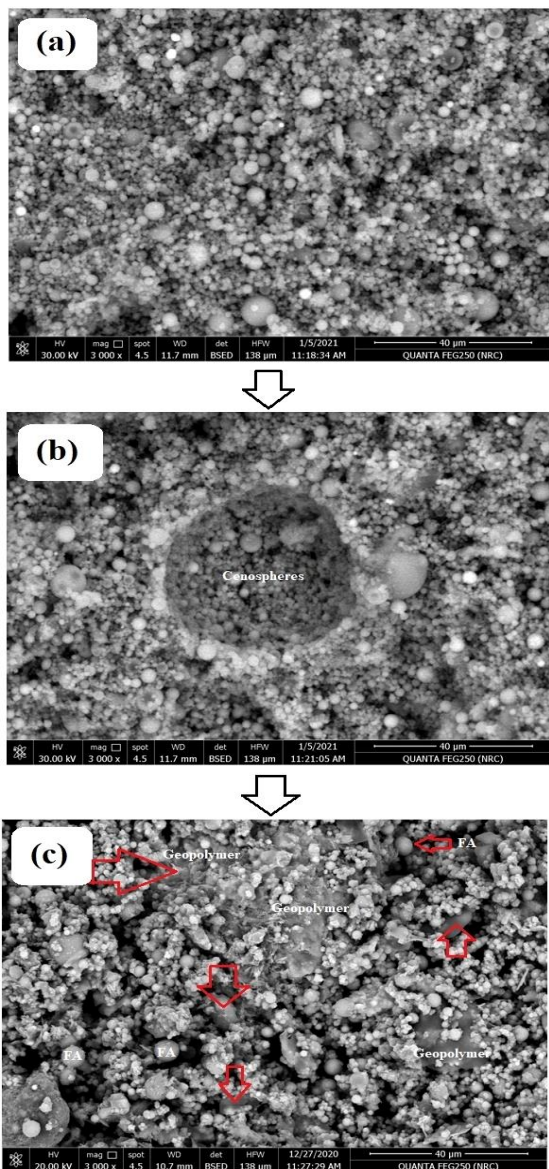


Figure 4. FE-SEM micrographs of: a) raw fly ash sample, b) primary activated fly ash by NaOH solution, c) the new formed geopolymer within the fly ash matrix.

Table 2: Water absorption and apparent porosity values of the studied mortars

Property		Mortar type		
		Geopolymer	Geopolymer+Lime	Geopolymer+TEOS
Water absorption (%)	After curing	10.5	9.54	8.7
	After salt weathering	11.9	10.4	9.1
Apparent porosity (%)	After curing	16.3	13.4	12.4
	After salt weathering	18.1	14.3	13.8

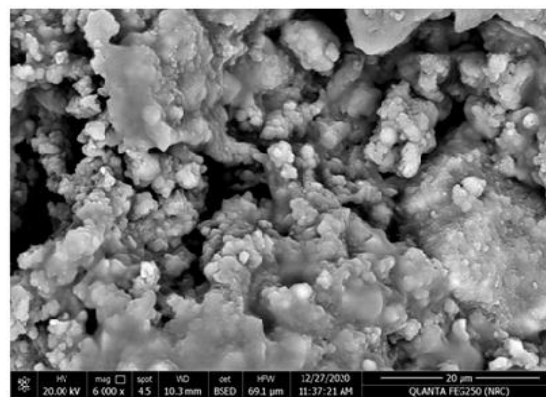


Figure 5. FE-SEM micrograph of the produced gel after geopolymerization and the adding of TEOS.

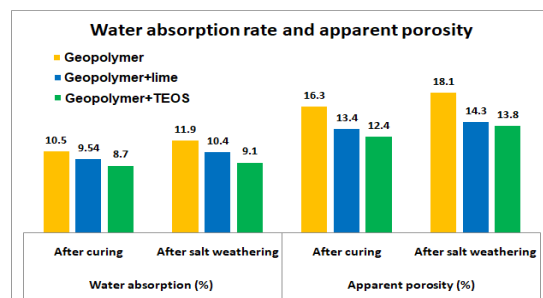


Figure 6. Values of the water absorption and apparent porosity of the tested mortars.

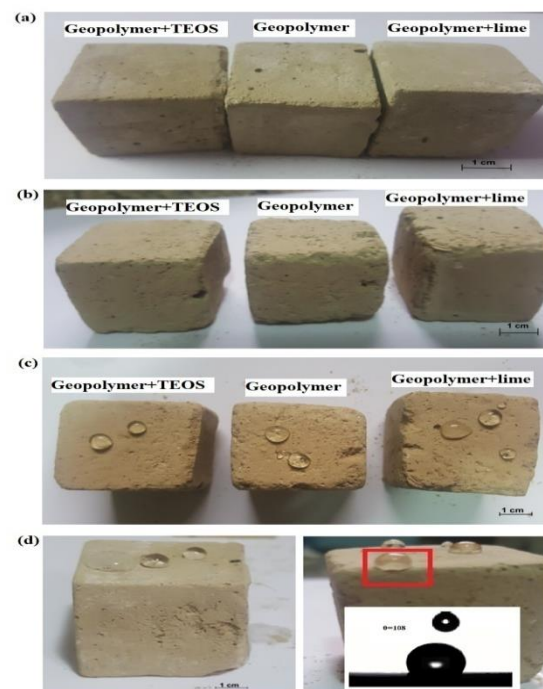


Figure 7. The outer appearance and water-repellent properties of the tested mortars: a) the mortar cubes after the complete curing, b) appearance of the cubes after thermal ageing at 110°C for 72 hrs., c) the hydrophobicity of the mortars, d) high resistance to wettability of the geopolymer+TEOS mortar.

Table 3: Bond and compressive strength values and shrinkage (%) of the studied mortars

Mortar/ Bond strength ($\times 10^{-2}$ N/mm ²) after curing			
	Geopolymer	Geopolymer+Lime	Geopolymer+TEOS
1 week	4.1	4.3	4.7
2 weeks	4.4	4.7	5.8
28 days	4.9	5.5	6.1
Bond strength ($\times 10^{-2}$ N/mm ²) after salt solution wet/dry cycles			
1 cycle	3.9	4.1	4.3
10 cycles	3.7	3.8	3.9
15 cycles	3.3	3.6	3.7
Compressive strength (MPa)			
After curing	25.1	31.4	28.5
After salt weathering	24.2	29.6	27.5
Shrinkage (%)			
Days			
0	0.13	0.14	0.1
15	1.33	1.4	1.3
21	1.7	2.2	1.6
30	2.1	2.3	2
60	2.3	2.4	2.34

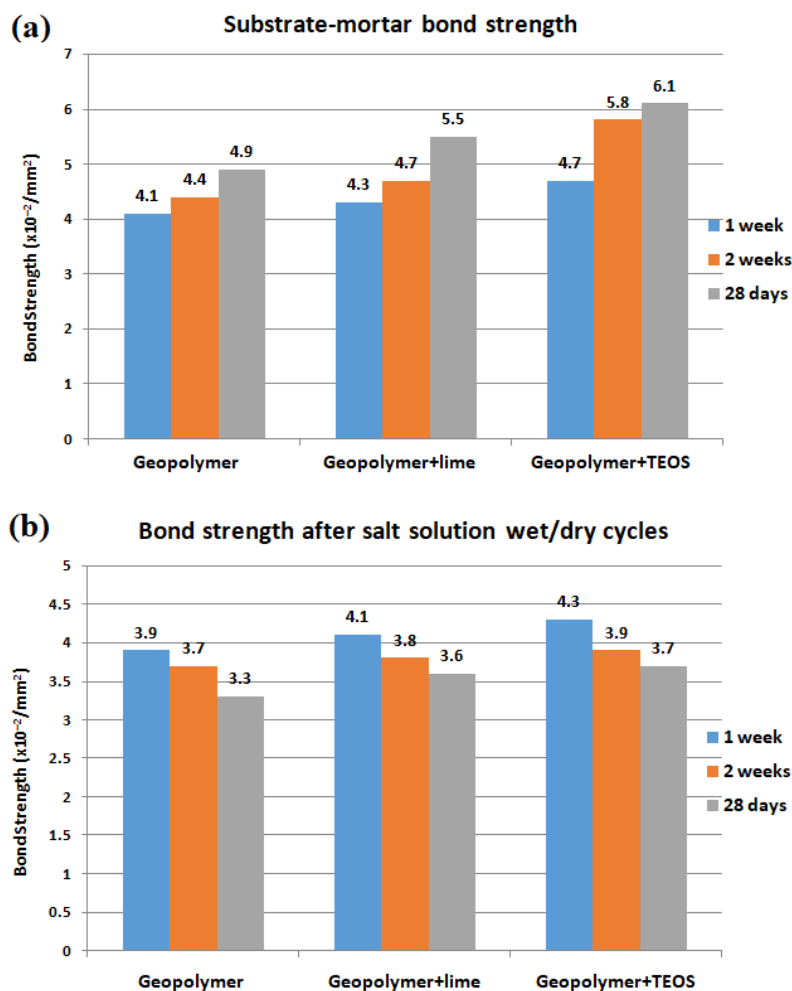


Figure 8. Bond strength values of the studied mortars before and after salt weathering.

After salt weathering, the geopolymer mortar showed the biggest bond strength difference (8.3%), from the 1st cycle to the 15th cycle, followed by the geopolymer+TEOS mortar (7.5%)

(Fig. 8b). While the lowest change was reported for the geopolymer+lime mortar (6.49%). In contrast to the physical properties of the lime+geopolymer mortar, a notable compressive strength (CS) was

reported (31.4 MPa). Probably, this mechanical advantage is related to the compactness of the high alkali binder in the microstructure of the formula [19]. However, the geopolymer specimens showed the lowest value (25.1 MPa) (Fig. 9a). Worthy to report that the highest (CS) values were achieved after the complete curing of the mortars. For all mortars, a slight decrease in the compressive strength was occurred after salt weathering.

3.6. Evaluation of the shrinkage percentage

The shrinkage of mortar is a key factor which reflects its volume stability and workability. The

change in shrinkage was reported over 60 days. Directly after preparing the mortars, no significant shrinkage was measured, while remarkable values were registered after 30 and 60 days (Table 3& Fig. 9b). Within two months, the mortars gave values of 2.3, 2.4 and 2.34%, respectively. Worthy to report that the biggest difference, from the time of casting and after 30 and 60 days, was registered for the geopolymer+TEOS mortar (91.8%), followed by the geopolymer mortar (89%). While the geopolymer+lime mortar showed the lowest percentage (88.9%).

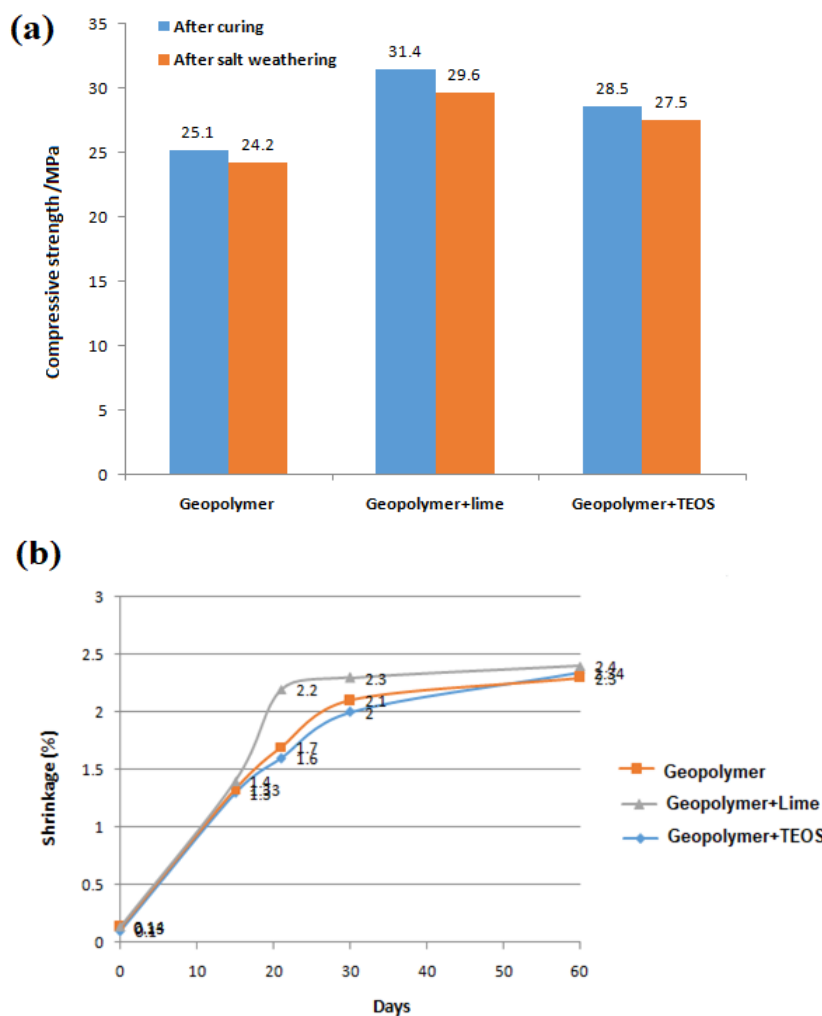


Figure 9. a) the compressive strength values before and after salt weathering, b) the shrinkage curve of the tested mortars.

3.7. Workability

A grout formula of the geopolymer and hydrated lime (3 parts:1 part, by weight) was prepared. Hydrated lime helps in improving the flexibility and increasing the water retention which ensure good adhesion properties to the mortar. In order to insure the fluidity of the tested grouts, sodium gluconate $\text{NaC}_6\text{H}_{11}\text{O}_7$ (1 part per weight) was added to the mortar formula. The initial flow rate

was evaluated according to the ‘‘EN 459-2 standard’’. The fluidity rate is usually measured by a capillary viscometer (e.g. Brookfield viscometer).

In Figure (10), the grout viscosity was evaluated, in correlation to the percentage of the water-reducing agent (sodium gluconate). It was found that a low viscosity was resulted by adding a percentage of 1% sodium gluconate, with value around 30 centipoise (cP) (30 mPa·s).

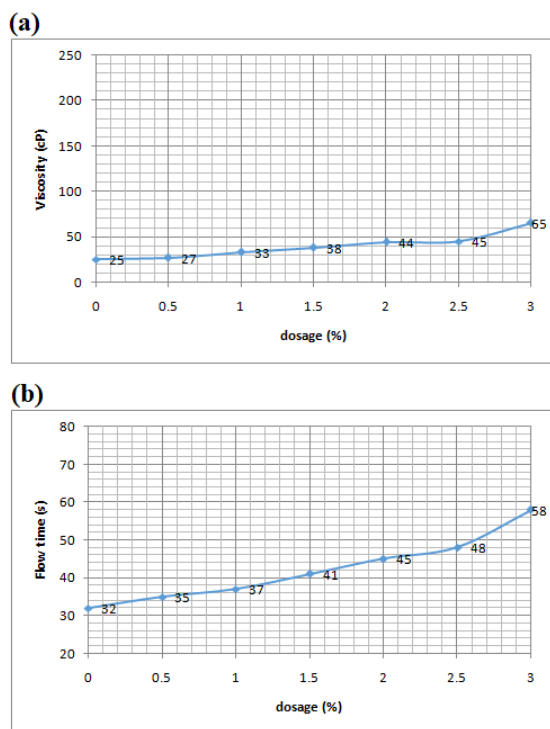


Figure 10. The viscosity values and flow time rate of the tested grout.

By increasing the sodium gluconate up to 3%, the plasticity of the grout was affected dramatically, giving a viscosity value of 65 cP (65 mPa·s). In case of the sensitive mud plasters, the adding of sodium gluconate to the grout admixtures reduces the amount of the mixing water. While, the flow time of the grout, determined for 500 mL, is ranging between 30 and 60 s.

3.8. Stability in a saline medium

Salt weathering affects wall paintings in many archaeological sites in Egypt. International testing standards usually apply salt test to evaluate the stability of materials under aggressive conditions. The mortar cubes were subjected to cycles of drying/immersion in a saline solution (10% NaCl in water). Each single cycle included 2 hrs drying in an oven at 110°C, followed by an immediate immersion of the cubes in a saline solution for 8 hrs. The described cycle was repeated for 15 times. The visual examination of the samples showed a great resistance of all mortars together with undetectable colour change and micro loss of the cubes mass. During immersion, a notable stability against wetting was reported in case of the geopolymer+TEOS mortar.

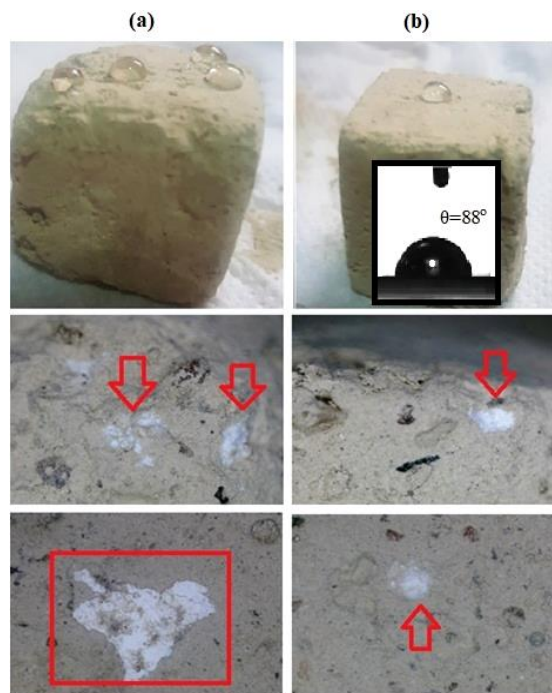


Figure 11. The water repellent features of the cubes after salt weathering: a) geopolymer, b) geopolymer+TEOS composite.

The weight of cubes was registered for each accelerated ageing cycle. It was noticed that no significant loss of the cubes was occurred. But, a slight erosion of the edges was found after the 11th cycle. Also, few patches and salt nodules were deposited inside the mortar matrix. As observed in Figure (11), the water repellent features of the cubes have not been seriously affected by salt weathering, both for the geopolymer mortar (Fig.11a) and the geopolymer+TEOS mortar (Fig. 11b).

4. Discussion

The results showed the positive reflection of the formed geopolymer for multipurpose restoration applications. It should be noted that the manufactured geopolymer achieved low apparent porosity and water absorption values. The highest apparent porosity value was reported for the geopolymer (16.3%), probably due to the high amount of the unreacted particles in the microstructure. According to Canakci et al. [20], unreacted particles are occurred due to the failure, or incomplete reaction, during the alkali activation. A significant reduction of the measured values was found by adding TEOS to the geopolymer [21]. The geopolymer mortars were tested for bond and compressive strength. The geopolymer+TEOS mortar reached the best bond strength after 28 days (with a value of 6.1 N/mm²). After salt weathering, the mortars approved a high resistance to etching. The hydrophobic properties remained

unchangeable even after the cycles of drying and immersion in the NaCl solution.

By reviewing the compressive strength values of the studied mortars, the geopolymer+lime showed the highest value (31.4 MPa). More, it expressed a high stability after salt weathering with a value of 29.6 MPa. Hardjito et al. [22] noticed that the compressive strength values of the geopolymer mortars become greater by increasing the curing temperature and reaching the final setting time. According to Kaur et al. [23], the molar concentration of NaOH affects positively the durability of the geopolymer mortars. The authors claimed that the maximum (CS) values were reported after the complete curing (after 28 days). This is probably due to the high alkaline content of the mortar (of NaOH and $\text{Ca}(\text{OH})_2$) which played a vital role in the geopolymerisation process and consequently, the mechanical improvements of the mortars. In a recent research by Abdel Salam et al. [24], the role of curing time and NaOH molarity on the geopolymer polymerization was discussed. Abdelmawla et al. [25], documented the high compressive strength resulted from the reaction of dealuminated metakaolin with sodium hydroxide.

In our case, a slight shrinkage of the tested mortars was reported after 30 and 60 days. The highest change, with a percentage of 2.4%, was achieved by the geopolymer+lime. As suggested by Norkhairunnisa and Muhammad Fariz [26], the shrinkage behaviour is highly affected by the Si and Al ratios in the used fly ash, and also by adding expansion agents.

An injection grout formula was tested to evaluate its workability to repair detached plaster layers. The grout was prepared using geopolymer, hydrated lime and sodium gluconate. Pasian et al. [27] mentioned that the injection grouts should fulfil enough compatible properties to the original substrates. The viscosity and flow rate values of the tested grouts were in an acceptable range (between 30 and 60 s). Further, the results have shown that a percentage of 3% sodium gluconate will ensure enough plasticity and good cohesion. Actually, these observations were adequate to allow good injectability and pumpability of the grout [28, 29].

5. Conclusion

The geopolymer formulas designed in this research by the activation of fly ash (FA) with sodium hydroxide (NaOH) showed promising results for repairing the damaged ancient wall paintings. The suggested mortars have successfully achieved physical and mechanical enhancements. The tested mortars achieved low water absorption and apparent porosity. The highest bond strength was documented for the geopolymer+TEOS, while the best compressive strength was attained by the

geopolymer+lime. Further, a hydrophobic feature was observed for all mortars. Compared to the tested mortars, the geopolymer-tetraethyl orthosilicate-TEOS composite showed the lowest wettability, but it showed a noticeable shrinkage. A grout mortar based on the produced geopolymer together with hydrated lime was evaluated. By the application of sodium gluconate, the viscosity and plasticity were promoted. It was confirmed through the laboratory salt weathering that the tested mortars have a high stability.

In principle, this research emphasises the compatibility of applying a geopolymer composite with tetraethyl orthosilicate or hydrated lime as repair mortars in the field of wall paintings restoration inside the rock tombs. This study recommends the use of geopolymers to fill the rock joints and to reduce the defects of stone supports in the rock tombs. Further, the mortar is durable and suitable for application to monuments that exist in aggressive environments (coastal, desert, etc.). For practical application, the colour tonality and geopolymer amount are depending on the physical-mechanical properties of the original materials for each object.

References

- [1] Wong, L., Rickerby, S., Rava, A. and Sharkawi, A.E.M. Developing approaches for conserving painted plasters in the royal tombs of the Valley of the Queens. In: *XIth International Conference on the Study and Conservation of Earthen Architecture Heritage (Terra 2012)*, 22-27 April 2012, Lima, Peru, pp. 1-14.
- [2] Mackay, E. The Cutting and Preparation of Tomb-Chapels in the Theban Necropolis. *The Journal of Egyptian Archaeology*, **7**(3-4), 154-168 (1921). Doi: [10.2307/3853562](https://doi.org/10.2307/3853562)
- [3] Bader, N.A. The deterioration problems of the wall reliefs of Komir temple, Esna, Egypt. *Mediterranean Archaeology and Archaeometry*, **14**(1), 201-219 (2014).
- [4] Ahmed, M.A., Ali, M.F., Bader, N.A. and Khalaphallah, R. The effect of wild pigeon excreta on the wall painting of Ramses III temple at Medinet Habu, Luxor. *SCIENTIFIC CULTURE*, **7**(3), 53-63 (2021).
- [5] Ali, M.F., El-Shafey, H. and Marey Mahmoud, H. Multianalytical techniques of Al-Bīmāristān Al-Mu'ayyidi mural painting at historic Cairo: contribution to conservation and restoration, *SCIENTIFIC CULTURE*, **7**(2), 33-47 (2021).
- [6] Majidi, B. Geopolymer technology, from fundamentals to advanced applications: a review. *Materials Technology*, **24**(2), 79-87 (2009). Doi: [10.1179/175355509X449355](https://doi.org/10.1179/175355509X449355)
- [7] Moon, J., Bae, S., Celik, K., Yoon, S., Ki-Hyun, K., Kim, K.S. and Monteiro, P.J.M. Characterization of natural pozzolan-based geopolymeric binders. *Cement and Concrete Composites*, **53**, 97-104 (2014).

- Doi:<https://doi.org/10.1016/j.cemconcomp.2014.06.010>
- [8] Palomo, A., Grutzeck, M.W. and Blanco, M.T. Alkali-activated fly ashes A cement for the future. *Cement and Concrete Research*, **29**, 1323-1329 (1999).
- [9] Fadel, O., Hekal, E.E., Hashem, F.S. and Selim, F.A. Mechanical Properties, Resistance to Fire and Durability for Sulfate Ions of Alkali activated Cement made from Blast Furnace Slag-Fine Metakaolin. *Egyptian Journal of Chemistry*, **63**(12), 4821-4831 (2020).
- [10] Somna, K., Jaturapitakkul, Ch., Kajitvichyanukul, P. and Chindaprasirt, Ch. NaOH-activated ground fly ash_geopolymer cured at ambient temperature. *Fuel*, **90**(6), 2118-2124 (2011).
Doi: <https://doi.org/10.1016/j.fuel.2011.01.018>
- [11] Clausi, M., Magnani, L.L., Occhipinti, R., Occhipinti, R., Riccardi, M.P., Zema, M. and Tarantino, S.C. Interaction of metakaolin-based geopolymers with natural and artificial stones and implications on their use in cultural heritage. *International Journal of Conservation Science*, **7**(2), 871-884 (2016).
- [12] Ricciotti, L., Molin, J. A., Roviello, V., Chianese, E., Cennamo, P. and Roviello, G. Geopolymer Composites for Potential Applications in Cultural Heritage. *Environments*, **4**(4), 91 (2017).
Doi:[10.3390/environments4040091](https://doi.org/10.3390/environments4040091)
- [13] Pagnotta, S., Tenorio, A.L., Tinè, M.R. and Lezzerini, M. Geopolymer mortar: metakaolin-based recipe for Cultural Heritage Application, In: *International Conference on Metrology for Archaeology and Cultural Heritage (2020 IMEKO TC-4)*, Trento, Italy, October 22-24, 2020, pp. 55-59.
- [14] Occhipinti, R., Stroschio, A., Finocchiaro, C., Fugazzotto, M., Leonelli, C., Lo Faro, M.J., Megna, B., Barone, G. and Mazzolenia, P. Alkali activated materials using pumice from the Aeolian Islands (Sicily, Italy) and their potentiality for cultural heritage applications: preliminary study. *Construction and Building Materials*, **259**, 120391 (2020). Doi: [10.1016/j.conbuildmat.2020.120391](https://doi.org/10.1016/j.conbuildmat.2020.120391)
- [15] El Khomsi, A., Gharzouni, A., Farges, R., Dupont, P., Kandri, N.I., Zerouale, A. and Rossigno, S. Geopolymer Composite Coatings Based on Moroccan Clay and Sands for Restoration Application. *Frontiers of Chemical Science and Engineering*, **3**, 667982 (2021).
Doi: [10.3389/fceng.2021.667982](https://doi.org/10.3389/fceng.2021.667982)
- [16] Roviello, G., Ricciotti L., Molino, A.J., Menna, C., Ferone, C., Cioffi, R. and Tarallo, O. Hybrid Geopolymers from Fly Ash and Polysiloxanes. *Molecules*, **24**, 3510 (2019).
Doi:[10.3390/molecules24193510](https://doi.org/10.3390/molecules24193510)
- [17] dos Santos, A.R.L., da Silva Veiga, M. D.R., dos Santos Silva, A.M. and de Brito, J.M.C. Tensile bond strength of lime-based mortars: The role of the microstructure on their performance assessed by a new non-standard test method. *Journal of Building Engineering*, **29**, 101136 (2020).
Doi: <https://doi.org/10.1016/j.jobe.2019.101136>
- [18] Fernández-Jiménez, A., García-Lodeiro, I., Maltseva, O. and Palomo, A. Mechanical-Chemical Activation of Coal Fly Ashes: An Effective Way for Recycling and Make Cementitious Materials. *Frontiers in Materials*, **6**(51) (2019).
Doi: [10.3389/fmats.2019.00051](https://doi.org/10.3389/fmats.2019.00051)
- [19] Baltazar, L.G., Henriques, F.M.A., Temporão, D. and Teresa Cidade, M. Experimental Assessment of Geopolymer Grouts for Stone Masonry Strengthening. *Key Engineering Materials*, **817**, 507-513 (2019).
- [20] Canakci, H., Güllü, H. and Alhashemy, A. Performances of Using Geopolymers Made with Various Stabilizers for Deep Mixing. *Materials*, **12**, 2542 (2019).
Doi:[10.3390/ma12162542](https://doi.org/10.3390/ma12162542).
- [21] Mašek, Z. and Diblíková, L. Hydrophobic impregnation of Geopolymer composite by Ethoxysilanes. *Acta Polytechnica*, **58**(3), 184-188 (2018).
Doi: [10.14311/AP.2018.58.0184](https://doi.org/10.14311/AP.2018.58.0184)
- [22] Hardjito, D., Chung Cheak, Ch. and Lee Ing, C.H. Strength and Setting Times of Low Calcium Fly Ash-based geopolymer mortar. *Modern Applied Science*, **2**(4), 3-11. (2009).
Doi: [10.5539/mas.v2n4p3](https://doi.org/10.5539/mas.v2n4p3)
- [23] Kaur, M., Singh, J. and Kaur, M. Synthesis of fly ash based geopolymer mortar considering different concentrations and combinations of alkaline activator solution. *Ceramics International*, **44**, 1534-1537 (2018).
- [24] Abdel Salam, N.F., Ghaly, S.T., Abadir, M.F. and Amin, Sh. K. Preparation of Geopolymer Bricks from Alum Waste. *Egyptian Journal of Chemistry*, **65**(2), 71-80 (2022).
- [25] Abdelmawla, M., Abdelaa, A., Beheary, M.S., Abdullah, N.A. and Razek, T.M.A. Solidification of Alum Industry Waste for Producing Geopolymer Mortar. *Egyptian Journal of Chemistry*, **63**(11), 4285-4294 (2020).
- [26] Norkhairunnisa, M. and Muhammad Fariz, M. N. Geopolymer: A review on physical properties of inorganic aluminosilicate coating materials. *Materials Science Forum*, **803**, 367-373 (2015).
- [27] Pasian, Ch., Secco, M., Piqué, F., Artioli, G., Rickerby, S. and Catherg, Sh. Lime-based injection grouts with reduced water content: An assessment of the effects of the water-reducing agents ovalbumin and ethanol on the mineralogical evolution and properties of grouts. *Journal of Cultural Heritage*, **30**, 70-80 (2018).
- [28] Azadi, M.R., Taghichian, A. and Taheri, A. Optimization of cement-based grouts using chemical additives. *Journal of Rock Mechanics and Geotechnical Engineering*, **9**, 623-637 (2017).
- [29] Vavricůk, A., Bokan-Bosiljkov, V. and Kramar, S. The influence of metakaolin on the properties of natural hydraulic lime-based grouts for historic masonry repair. *Construction and Building Materials*, **172**, 706-716 (2018).
Doi:<https://doi.org/10.4028/www.scientific.net/MSF.803.367>